"Cut-Glue" Approximation Method for Strongly Nonlinear and Multidimensional Object Dependencies Modeling

Rudolf Neydorf, Anna Neydorf and Dean Vučinić

Abstract The main difficulties in modeling a variety of technical systems are experienced when creating appropriate mathematical objects to simulate their behavior. It is well known that such inter-objects dependences are defined with their variable with strong nonlinear and multidimensional characteristics. The mathematical models (MM) dependences are approximated with advance numerical methods, such as polynomial decomposition, spline functions, etc., which are today still very time-consuming and laborious to be correctly created and applied, also considering their precision. In this paper, the authors have created and investigated the high-precision analytical approximation method to model the nonlinear MM dependences, which are defined only by appropriate analytical functions. These approaches have been already studied in details, where the Cut-Glue approximation method defines 1-dimensional dependences, and to 2-dimensional dependences were approximated with analytical functions of 2 arguments. The important advantage of the Cut-Glue method is that it well approximates the differentiability of the proposed MM dependencies, as its enables to investigate analytically the related modeling functions and thus, use them efficiently in applying MM in dynamical systems simulations. In this work, the Cut-Glue method has been further developed: (1) to prove its applicability by creating nonlinear models of any dimension, (2) to analyze its performance at all the stages, in which the "Cut-Glue" approximation is applied, and (3) to implement this formal algorithm, which allows numerical verification and validation of its applicability. The considered optimization criteria for both respective issues, accuracy and complexity, have been applied to the investigated MM-s. The proposed method is formalized by the optimal splitting of its experimental dependence into separate parts, which are then

R. Neydorf (✉) · A. Neydorf
Don State Technical University, Rostov-on-Don, Russia
e-mail: ran_pro@mail.ru

A. Neydorf
e-mail: neydan@yandex.ru

D. Vučinić
Vrije Universiteit Brussel, Brussel, Belgium
e-mail: dean.vucinic@vub.ac.be

A. Öchsner and H. Altenbach (eds.), *Improved Performance of Materials*,
Advanced Structured Materials 72, DOI 10.1007/978-3-319-59590-0_13

numerically defined and implemented within the proposed software, developed in this work. In this paper, the different possibilities of applying the optimal multi-dimensional "Cut-Glue" approximation method are illustrated by examples. The achieved results represent a strong base to significantly expand the proposed method applicability, and further on, they indicate potential opportunities to improve the existing solutions. Especially, when solving a variety of problems, which requires mathematical modeling of any type of technical objects, to simulate overall systems dynamics.

Keywords Optimization · Approximation · Mathematical modeling · Experimental data · Heuristic methods · Particle swarm optimization

1 Introduction

The experimental creation of the mathematical models (MM) of various processes, objects, systems, etc. requires information on the involved research object, which are described with data having a certain structure. The general structure of the experimental data for the created MM is represented with the K records, containing 2 lists: (1) entrances $(x_1, \ldots x_n)$ and (2) exits $(y_1, \ldots y_m)$. Such structure implies that K is the number of the experiment tests, x_i is the independent variables, y_j—dependent variables. The dependency modeling of the static variables of MM means that each output of y_j is the function of inputs $(x_1, \ldots x_n)$. In this case, each dependency is defined with a function φ_j, and general MM is defined by the Y vector function:

$$\left.\begin{aligned} y_j &= \varphi_j(x_1, \ldots x_n), \quad j = \overline{1, m}; \\ Y &= \Phi(x_1, \ldots x_n) = (y_1, \ldots y_m)^{\mathrm{T}}. \end{aligned}\right\} \tag{1}$$

In addition to the general structure of the experimental data, it is necessary to consider their internal structure. When carrying out a passive experiment, this structure can be order-less, which means that the entrance data lists are formed in a random way, and are not connected with each other, thus through defined dependences. When carrying out the experiment, usually, the input data are built on the regular basis. Then, *n-ki* (the vector or the sequence having *n* elements) of input variables is connected by the internal dependency, where their values and change of variables acquire a quite regular character. Most often, the so-called coordinate-wise principle for the variables variation in an experiment is used. The example of such an experiment creation is given in Table 1.

In this case, the force F_x of the side offset of the airship is the output variable, which is interesting to the researcher performing the experiment. The experimental results indicate that there is an influence on this force, which is coming from certain airship flight parameters, which are: height h, angle of heel α, and airship takeoff

Table 1 The dependences of the strength of the lateral airship displacement resulting from the flight parameters

Speed of rise	Altitude of fly	Angle of heel, α, angle degree					
		0	15	30	45	60	75
v, *m/s*	*h*, *km*	*F*(*h*), *kN*					
2.5	0	0.086	11.90	19.26	21.89	9.491	3.625
	5	0.050	6.996	19.12	13.03	5.422	2.871
	10	0.027	4.193	10.39	7.234	3.081	2.513
	15	0.012	1.957	4.707	3.382	1.435	0.720
4	0	0.224	30.19	46.28	57.61	22.88	12.44
	5	0.132	20.44	47.45	33.85	14.27	9.331
	10	0.071	12.30	27.24	18.54	8.056	5.605
	15	0.032	5.010	11.37	8.684	3.530	2.061
5	0	0.366	35.65	87.22	87.99	36.68	25.84
	5	0.208	26.47	67.39	52.48	23.09	17.01
	10	0.113	22.48	42.77	28.84	12.30	8.501
	15	0.051	7.841	17.72	13.77	5.482	2.238
6	0	0.550	61.54	119.43	127.3	58.23	37.38
	5	0.300	36.71	96.68	77.62	32.76	22.34
	10	0.166	22.96	60.82	41.88	19.97	11.48
	15	0.074	11.35	25.56	19.89	8.192	4.371
7.5	0	0.894	80.35	180.3	185.4	92.46	55.31
	5	0.480	79.17	133.1	123.3	50.86	27.49
	10	0.261	42.74	84.90	66.40	28.04	24.42
	15	0.117	18.24	44.90	30.76	13.34	8.445

speed *v*. These parameters are acquired from the flight experiment through the limited number sequences. As a result, for 2-dimensional dependences, it is possible to use the matrix-vector data representation. However, for 3-dimensional data, as an example given in Table 1, it is necessary to define a 3-dimensional matrix, to represent its structure. In general, these data can be displayed only by several matrixes, having chosen the fixed 3rd parameter for each matrix. Such data are presented in Table 1: 5 matrixes of dimension 4 × 6—with varying h and α, and with 5 values of speed. It can be noted that the smooth structure of the approximated dependences doesn't create difficulties when applying the mathematical methods.

However, this approach can be significantly more difficult when the data is not smooth, and has a fragmentary structure. The "fragmentary structure" has a piecewise nature, where the mutual change of the specific arrangement is represented with the pointwise data, making it possible to allocate certain sites (the differing sites of the approximation surface) with the obvious dependency, where the fragments can have significantly various inclinations through their contact lines. The example of the "fragmentary structure" of dependences is quite well illustrated

by the data shown in Table 1. The tabulated or matrix representation does not always allow estimating this characteristic, while the graphic form, as presented in Fig. 1, made this property more visible.

In these cases, the applied various methods are capable to fulfill the required accuracy, which guarantee the sufficient condition to have a solvable task, thus to receive the mathematical description for such nonlinearities. The piecewise approximation [1–3], in which dependence fragments are accepted as "pieces", is quite the simplest and the most efficient manner to cope with a problem of the data fragmentation. This method is applicable for any required approximation accuracy, but unfortunately, it has an important shortcoming. The discontinuities of the derivatives, arising on the lines, which are joining the fragments, are not defined as the analytical transformations of the related approximations. In that case, the spline approximation is more effective and closest to the piecewise approximation, for the mathematical description of the essential nonlinearities [4–6]. However, this approach considerably complicates the MM analytical transformation.

The regression analysis [7–10], the numerous methods applying special polynomial decompositions [11–13], radial basis functions [14–16], etc. are related to them. However, these methods are not adapted to approximate the piecewise dependences, as they do not provide sufficient accuracy [7–13], or they are focused on the description and representation of the graphical images [14–16].

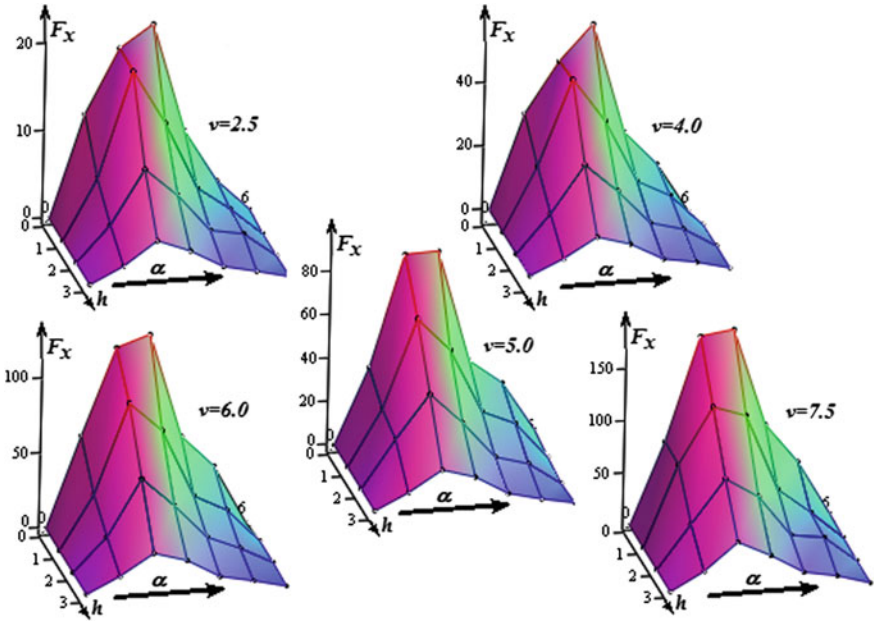

Fig. 1 2-dimensional fragments for arguments $-\alpha$, defined for $4h$ values defining 3-dimensional piecewise experimental dependences

2 Basic Provisions and Boundaries for Application of "Cut-Glue" Approximation

For elimination of the specified shortcomings the cut-glue approximation method has been developed [17–19]. The method allows presenting the piecewise dependences with one analytical function, which has an additive structure consisting of multiplicative members. These members perform the multiplication of 2 functions: (1) the function approximating some fragment (FAF) of dependence, and (2) the function, which multiplicatively is cutting out this fragment (MCF).

The multiplication of FAF and IMF provides two results: (1) the FAF values within the fragment borders remain almost invariable, (2) all values of the multiplicative member behind the "cut-out" fragment borders become almost zero. The obtained result is the interval, which is isolating the analytical function (IIF) [17, 18]. The analytical property of IIF enables the algebraic addition of the multiplicative members, having the smooth piecewise dependency approximation with the improved accuracy, peculiar to IIF. At the same time, the coefficient of the parametrical identification ε, which is one of the MCF arguments, allows in addition, to adjust the general accuracy of the approximation. This function represents the united approximating function (UAF), which mathematically describes all the experimental data. At the same time, the coefficients of the parametrical identification ε, as arguments of MCF, in addition, allow to adjust the accuracy of the approximated data with the use of UAF.

In articles [17, 18], the bases of the cut-glue approximation for the solution of 1-dimensional tasks are developed. In article [19] this method is generalized for the 2-dimensional case. Often, there is a need to approximate the multidimensional dependences [1, 4, 9, 10, 19–24]. For example, the strength properties of the composite materials depend both, on the concentration of components, and on technological parameters of their production [26–28]. The positioning of the robot multilink working body is also described by multidimensional nonlinear dependences. For some positions, the relative bodies positioning has a discontinuity in their mathematical description [23, 29, 30]. In order to finalize the solution in a case of the nonlinear object control, only the mathematical model description is not sufficient, as it needs to contain the analytical functions to describe its dependencies, which synthesize the control law this object [30, 31, 32].

For example, in work [22], a similar dependence is represented as in Fig. 1 for the 2-dimensional MM, which is received from the cut-glue approximation. The model describes the communication of the airship moment from the side heel, with the climbing speed (v, m/s) and with angle of the heel (α, angular degrees). However, the dependence is 3-dimensional, as illustrated in Table 1, and shown with the 3D images in Fig. 1, where this dependence has the 3rd state variable—flight altitude (h, km), which is added up to the 2 already specified state variables. The 2-dimensional cuts of the modelled dependence are constructed in Fig. 1, and have obvious breaks along the dividing lines. The nature of dependence change is not resulting from the experiment error. It is caused by the breakaway of the air

stream, which flows around the airship at certain combinations of v, α and density of air, largely depending on h. In operation [22] it was succeeded to describe such dependence function of 2 variables, with fulfilling the acceptable accuracy, only by the cut-glue approximation. To define a similar dependence, by involving 3 variables, is becoming a much more complex problem. Therefore, to solve the 3-dimensional problem, it is necessary to adapt the "cut-glue" approach to find a solution for the bigger dimension problem.

3 Problem Formulation

In this article, the possibility to define the mathematical description and the related experimental dependences for any n-dimension, by applying the "cut-glue" approximation method, as developed in [17–20] is analyzed. In other words, it is necessary to assert the general approach for the creation of the uniform analytical differentiable function, which can describe any nonlinear dependence, including the discontinuous derivatives. According to the "cut-glue" approximation, the method has to be realized with use of the multiplicative "cutting out" of n-dimensional fragments, modeled with the n-dimensional surface. The fragments need to have the general mutual borders, providing the full range coverage of the approximated dependences. The general uniform MM with the approximated dependences has to associate the created fragments by applying the algebraic summation.

4 Experimental Fragmentation of Multidimensional Strongly Nonlinear Dependencies

The process of the fragmentation is connected with the sufficient allocation of smooth sites dependence to each coordinate. This process is very difficult, as in many cases the dependence curvature can significantly change, due to the variation influenced with other coordinates. Such property of the multidimensional dependences is well visible in the 3D images, as shown in Fig. 1.

Usually, such dependences are dividing intervals, based on the respective variable. To make it more visual appealing in the multidimensional case, even for 3-dimensional dependence, it is quite difficult to achieve it. For example, the above described 3-dimensional dependence $F_x(v, h, \alpha)$, is illustrated in Table 1 by numerical values, and shown in Fig. 1. It is demonstrated by the 3D—projections, which are constructed in the plane of arguments $h - \alpha$. The smooth curvature of the F_x dependency on the h argument, and the existence of breaks with the extremum are well visible for the same dependency on an argument α. However, it is difficult to estimate the nature of its curvature depending on the v argument.

It is possible to reconstruct the table and 3D-projections in the plane with the $v - \alpha$ arguments, in order to achieve the visual assessment. Then, the 3D-projections of $F_x(v, h, \alpha)$ are done on this plane and for the matrixes, and by fixing h it is possible to estimate the nonlinearity influence of h on F_x. Besides that, during the regular creation of the coordinates grid, the experiment entrance data can be submitted as a multidimensional matrix. Thus, the data of Table 1 can be submitted by a 3-dimensional matrix, which sides are 2-dimensional matrixes, as shown in Fig. 2. However, both procedures are quite cumbersome. With the increase of the model dependencies dimension the complexity of the assessment of its properties in the factorial space, and respectively, the complexity of the fragmentation is increasing rapidly. Due to the revealed features of the fragmentation procedure for the experimental data with the multivariate dependences (for $n \geq 3$) it is worth to notice that the relevance of automation of the fragmentation procedure is an important software part. Without such software support, the cut-glue dependency approximation for 3 and more variables would not be achievable.

Despite the specified difficulties, for the presented multidimensional application of the "cut-glue" approximation for the 3-dimensional mathematical model with the $F_x(v, h, \alpha)$ dependency, resulting from the experimental data given in Table 1, has been defined and solved.

The 3-dimensional matrix in Fig. 2, where the red rectangles show the projections of the selected 3-dimensional fragments to «$v - \alpha$», «$h - \alpha$» and «$v - h$» planes (front, top and side of the 3-dimensional data matrix). The analysis of such

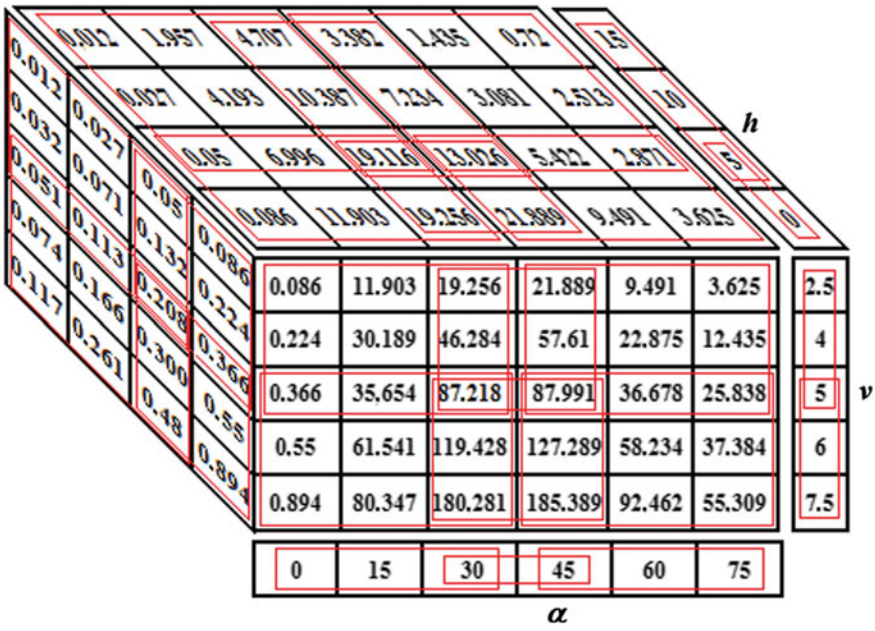

Fig. 2 3-dimensional fragmentation of the 3-dimensional piecewise experimental dependency

configurations for the allocated sub-matrixes shows that the presence of the coinciding peripheral areas, at the adjacent fragments, is in general having very law fragmentation. The dimension of a bordering subspace is always one dimension less than the dimension of the adjoining subspaces encompassing such multidimensional space of the basic data. The 2-dimensional surfaces (parallelograms) for the next 3-dimensional fragments (parallelepipeds) are coinciding. The 1-dimensional edges (intervals) of these parallelograms and 0-dimensional boundary points of these intervals are coinciding too.

The fragmentation of the data matrix is a consequence of the fragmentation of the vectors, which are constructed from the arguments values, which varied in an experiment to certain levels. In this case, the input variables vectors of an experiment $\overrightarrow{x_i}, i = \overline{1,n}$ are represented by a set of subvectors.

$$\overrightarrow{x_{i_j}}, i = \overline{1,n}, j = \overline{1,n_i}, \quad \text{where } \vec{x} = \begin{pmatrix} x_1 \\ \dots \\ x_n \end{pmatrix}; \ \overrightarrow{x_i} = \begin{pmatrix} x_{i_1} \\ \dots \\ x_{i_{n_i}} \end{pmatrix}. \tag{2}$$

In the fragmentation option presented in Fig. 2, these sub-vectors are defined as follows:

$$\overrightarrow{x_1} = \vec{h} = \begin{pmatrix} \overrightarrow{h_1} \\ \overrightarrow{h_2} \end{pmatrix}; \quad \overrightarrow{x_2} = \vec{v} = \begin{pmatrix} \overrightarrow{v_1} \\ \overrightarrow{v_2} \end{pmatrix}; \quad \overrightarrow{x_3} = \vec{\alpha} = \begin{pmatrix} \overrightarrow{\alpha_1} \\ \overrightarrow{\alpha_2} \\ \overrightarrow{\alpha_3} \end{pmatrix}; \tag{3}$$

$$\overrightarrow{h_1} = \begin{pmatrix} 0 \\ 5 \end{pmatrix}; \quad \overrightarrow{h_2} = \begin{pmatrix} 5 \\ 10 \\ 15 \end{pmatrix}; \quad \overrightarrow{v_1} = \begin{pmatrix} 2.5 \\ 4.0 \\ 5.0 \end{pmatrix}; \quad \overrightarrow{v_2} = \begin{pmatrix} 5.0 \\ 6.0 \\ 7.5 \end{pmatrix}; \quad \overrightarrow{\alpha_1} = \begin{pmatrix} 0 \\ 15 \\ 30 \end{pmatrix};$$
$$\overrightarrow{\alpha_2} = \begin{pmatrix} 30 \\ 45 \end{pmatrix}; \quad \overrightarrow{\alpha_3} = \begin{pmatrix} 45 \\ 60 \\ 75 \end{pmatrix}. \tag{4}$$

Thus, the 3-dimensional dependency data, provided in Table 1, are divided into 12 3-dimensional fragments of the experimental data (FED) represented, generally as parallelepipeds.

The further implementation stage, of the cut-glue approximation method, consists in approximating each FED by an analytic function of *N*- (in this case 3-) variables. The data approximation shall provide the required accuracy, which is set for such solvable data domain task, and within the respective fragment. This function is called above FAF, and behind a fragment borders the FAF values can be any, but excepting to support the exponential growth to infinity. As the method applies the polynomial equations of the regression, such property for FAF is not applicable.

5 Multidimensional Approximation of Fragments for Experimental Dependences

According to the paradigm of the cut-glue approximation method [17–19, 22], the approximation in each fragment is selected for all the experimental data of n-dimensions in the second stage of the method. The approximation of the fragments is defined with the analytical FAF of n-arguments $\vec{x} = (x_1, \ldots, x_n)'$. The defined n-FAF functions $y_{(i_1,\ldots i_n)}$ receive the approximated fragments. They are identified with n-tuplets indices, which indicate the fragment contribution in the R^n—space—$(i_1, \ldots i_n)$:

$$y_{(i_1,\ldots i_n)} = \varphi_{(i_1,\ldots i_n)}(\vec{x}). \tag{5}$$

where i_j is the number of the fragment interval on x_j axis.

The fragments partition of variables $\overrightarrow{x_i}$ is defined by formulas (2)–(4). For example, the fragment (2,1,3), and function—$y_{(2,1,3)}$ mean that the fragment receives the input from the intervals: [5,15] for h, [2.5,5.0] for v and [45,75] for α. The receiving FAF uses the classical regression analysis to approximate experimental data with the specified polynomial degree. Therefore, in the presented example, the 12 polynomial equations have to be resulting from this second stage. The order and structure of each equation is defined by the number of data entering to 'FED', and by the accuracy imposed by the studied subject domain. Since, for the creation of the regression equations, the standard software algorithms, sometimes called standard software packages, are used. Thus this aspect in this article is not considered. After receiving all the FAF-s (as described in the example: $y_{(1,1,1)} - y_{(2,2,3)}$ it is possible to progress with the realization of the 3rd stage of the cut-glue approximation method. This stage is the creation of the interval-isolated functions (IIF). For this purpose, and according to the CGA paradigm, the specially designed functions—MCF—are defined. They have a number of unique mathematical properties. Therefore, first of all, the structure and properties of MCF, which depend on the application domain—structure and properties of the received FAF are considered.

6 Multiplicative Cutting-Out Function, Its Types and Properties

The kernel of the multiplicative method, when isolating a 1-dimensional fragment (a jog) of FAF on the x_j axis, consists in the multiplication of the FAF with the special 1-dimensional MCF (1-MCF) [17, 18], which has the following form:

$$\lambda_{j_i}\left(x_j, x_{j_{i-1}}, x_{j_i}, \varepsilon\right) = 0.25 \cdot \sigma_l\left(x_j, x_{j_{i-1}}, \varepsilon\right) \cdot \sigma_r\left(x_j, x_{j_i}, \varepsilon\right) / \delta\left(x_j, x_{j_{i-1}}, x_{j_i}, \varepsilon\right), \quad (6)$$

where

$$\sigma_l\left(x_j, x_{j_{i-1}}, \varepsilon\right) = x_j - x_{j_{i-1}} + \sqrt{\left(x_j - x_{j_{i-1}}\right)^2 + \varepsilon^2};$$

$$\sigma_r\left(x_j, x_{j_i}, \varepsilon\right) = x_{j_i} - x_j + \sqrt{\left(x_{j_i} - x_j\right)^2 + \varepsilon^2};$$

$$\delta\left(x_j, x_{j_{i-1}}, x_{j_i}, \varepsilon\right) = \sqrt{\left[\left(x_j - x_{j_{i-1}}\right)^2 + \varepsilon^2\right] \cdot \left[\left(x_{j_i} - x_j\right)^2 + \varepsilon^2\right]}.$$

The multiplicative function has the following form

$$\lambda_{(i_1,\ldots i_n)}\left(\vec{x}, \vec{x}_{(i_1-1,\ldots i_n-1)}, \vec{x}_{(i_1,\ldots i_n)}, \varepsilon\right) = \prod_{j=1}^{n} \lambda_{j_i}\left(x_j, x_{j_{i-1}}, x_{j_i}, \varepsilon\right) \quad (7)$$

and represents the pulse in space of R^{n+1}. The pulse amplitude approaches to 1 inside a fragment, and behind the fragment boundaries, the value of n-MCF is almost equal to 0.

Thus, expression (7) represents the n-dimensional MCF, or n-MCF. According to the cut-glue approximation method [19, 22], and by using *n*-FAF (8) and *n*-MCF (7), and with applying the multiplicatively construct for the *n*-dimension IIF, called *n*-IIF, as follows:

$$f_{(i_1,\ldots i_n)}(\vec{x}) = \varphi_{(i_1,\ldots i_n)}(\vec{x}) \cdot \lambda_{(i_1,\ldots i_n)}\left(\vec{x}, \vec{x}_{(i_1-1,\ldots i_n-1)}, \vec{x}_{(i_1,\ldots i_n)}, \varepsilon\right). \quad (8)$$

The functions 1-MCF and 2-MCF are developed and investigated in articles [18, 19], and have a number of important properties. The functions *n*-MCF has these properties too. A number of quantitative characteristics of these properties depend on the IMF dimension. Besides, depending on the space dimension, the new properties are added. Therefore, the full set of the inherited and new *n*-MCF properties is given below.

6.1 Properties of n-MCF

(1) Function (7) is symmetric in the middle of the approximated fragment range

$$\overrightarrow{\mathrm{x}_{\mathrm{i}0}} = \left(\frac{\mathrm{x}_{1_{i-1}} + \mathrm{x}_{1_i}}{2}, \ldots \frac{\mathrm{x}_{j_{i-1}} + \mathrm{x}_{j_i}}{2}, \ldots \frac{\mathrm{x}_{n_{i-1}} + \mathrm{x}_{n_i}}{2}\right). \quad (9)$$

(2) Function (7) has only the maximum in a point $\overrightarrow{\mathrm{x}_{\mathrm{i}0}}$ depending on a set of its adjusting parameters $\left\{\mathrm{x}_{j_{i-1}}, \mathrm{x}_{j_i}, \varepsilon_j \middle| j \in [1, n]\right\}$ and 0 infimum in such set, as follows:

Table 2 The boundary values on the MCF borders for various functions dimensions

n	1	2		3		
Border	Curve segment	Polygon side	Polygon vertex	Polyhedron face	Polyhedron edge	Polyhedron vertex
Value	0.5	0.5	0.25	0.5	0.25	0.125

$$\overrightarrow{X_0} = \left\{ \vec{x} \middle| \sqrt{x_1^2 + \cdots + x_n^2} \to \infty \right\}. \tag{10}$$

(3) With reduction of the adjusting parameter ε, the functions (8) can accept the value, as much as close to 1 in any range $\left[\overrightarrow{x_{l-1}}, \overrightarrow{x_l}\right]$ set as follows:

$$\forall \vec{x}, \overrightarrow{x_{l-1}}, \overrightarrow{x_l} : \vec{x} \in \left]\overrightarrow{x_{l-1}}, \overrightarrow{x_l}\right[\to \lim_{\varepsilon \to 0} \lambda_{(i_1,\ldots i_n)}\left(\vec{x}, \vec{x}_{(i_1-1,\ldots i_n-1)}, \vec{x}_{(i_1,\ldots i_n)}, \varepsilon\right) = 1. \tag{11}$$

(4) Function (7) in the ranges $[-\infty, (\overrightarrow{x_{i-1}})]$ and $[(\overrightarrow{x-1}), \infty]$ can accept value extremely close to 0 as follows:

$$\forall \vec{x}, \overrightarrow{x_{l-1}}, \overrightarrow{x_l}, \varepsilon : \vec{x} \notin \left[\overrightarrow{x_{l-1}}, \overrightarrow{x_l}\right] \to \lim_{\left|\overrightarrow{\mathrm{x}}\right| \to \infty} \lambda_{(\mathrm{i}_1,\ldots \mathrm{i}_n)}\left(\vec{\mathrm{x}}, \vec{\mathrm{x}}_{(\mathrm{i}_1-1,\ldots \mathrm{i}_n-1)}, \vec{\mathrm{x}}_{(\mathrm{i}_1,\ldots \mathrm{i}_n)}, \varepsilon\right) = 0 \tag{12}$$

(5) Function (7) allocates the n-dimensional parallelepiped in the R^n space. Values of the IMF (7) at the border sides, edges, which are parts, tops and so forth of this n-dimensional parallelepiped, aspire at $\varepsilon \to 0$ to the sizes depending only on n. For $n = 1, 2, 3$ the limits for the border values are given in Table 2.
(6) Use of IMF (7) in formula (8) provides the approach to $f_{(i_1,\ldots i_n)}(\vec{x})$ to $\varphi_{(i_1,\ldots i_n)}(\vec{x})$ with any accuracy depending on ε (except regional sides, edges and tops).
(7) The function (10) is infinite number of times continuously differentiated, as well as any function with the fractional exponent of degree.

7 Illustrative Example Creating IIF with FAF and MCF

For the descriptive reasons the graphic representation of the 2-dimensional approximation is considered. FAF of the fragment with the experimentally modeled dependency is described by the polynomial function of the 3rd order, and received by the KRA method having 2 arguments:

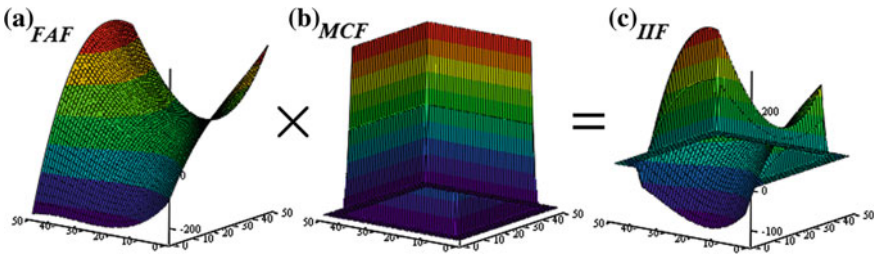

Fig. 3 Illustrate "cuttings" IIF from FAF by means of IMF; **a** FAF—analytical function approximation of fragment; **b** MCF—multiplicative cutting out function of fragment; **c** IIF —"isolated" function, describing only the fragment

$$z(x,y) = -108.91 - 66.87 \cdot x + 87.59 \cdot y + 10.5 \cdot x^2 - 3.25 \cdot x \cdot y - 7.741 \cdot y^2 - 0.52 \cdot x^3 + 0.98 \cdot x^2 \cdot y - 0.89 \cdot x \cdot y^2 + 0.37 \cdot y^3. \quad (13)$$

Its 3D image is shown in Fig. 3a. The borders of the fragment are determined by the intervals [5,45] with scales indicated on the horizontal axes. According to the drawing, it is visible that behind the fragment borders, the value of the approximating function, at the left and on the right is sharply increasing, and in the left frontal plane—sharply decreasing. However, it does not violate the conditions defining the FAF properties since function (13) is the polynomial. For "cutting out" the isolated IIF from FAF, the MCF is constructed by the use of formulas (6) and (7). This function has a parallelepiped representation, with top almost equal to 1 at the fragment borders, and almost 0 values outside these borders, see Fig. 3b. The horizontal axes in the 3D image are perpendicular to the paper page, i.e. the figure is shown as seen from the front and from below. The vertical axis is hidden behind IMF.

In Fig. 3, the multiplication of FAF and IMF allows to receive IIF—a basic element of "cut-glue" of approximation—are shown.

8 Additive Join of the Interval Isolating Functions into the Approximation United Function

The last stage of the cut-glue approximation method of *n*-dimensional data is to join the fragments constructed as IIF into one EAF function. Its role consists to approximate experimental data in the form of the analytical function—as united whole. The big advantage of this method is that such assembly is carried out by simple algebraic addition. The only condition to enable such combining is the explicit form of the output variable for all the IIF functions, which require the explicit form of their multiplicative components: FAF and IMF. The structure of

IMF is defined by formula (6), which is explicit form of the relatively $\lambda_{j_i}(*)$ function. The choice for FAF, to have the polynomial structure, provides its explicit character. Therefore, the EAF function completing the cut-glue approximation method can be defined as follows:

$$f(\vec{x}) = \sum_{i_1} \dots \sum_{i_n} f_{(i_1,\dots i_n)}(\vec{x}). \tag{14}$$

In other words the IIF "f" functions $f_{(i_1,\dots i_n)}(\vec{x})$ are added together coordinate-wise, and according to the coordinate-wise numbering of the fragments. The additive formation of EAF naturally inherits all the IIF properties, and, first of its analytical form, is the most important property of the "cut-glue" approximation method.

9 Illustrative Example of 3-Dimensional "Cut-Glue" Approximation Solution

The "cut-glue" approximation solution for the 3-dimensional data is given in Table 1 below. The full volume of the dependency data for the F_x force—the airship side shift—depends on the three flight parameters given in Table 1 angle of heel α, heights h and speed of its climbing velocity v is too complex for the demonstration of the approximation procedure to be put in this article. Therefore, the most important part of the studied characteristic containing its "hump", which is well visible in all the 5 3D-images shown in Fig. 1. Therefore, the most important part of the studied characteristic containing its "hump" requires fragmentation of the all the dependences, which require, at least 12 fragments. In this article, 4 fragments are described, as found to be the most important for covering the operational properties of the airship flight: $\alpha \in [0,60]$, $h \in [5,15]$, $v \in [2.5,7.5]$.

The data in Table 1 of the appointed range are highlighted in gray. The dependency form as shown in the 3D-images of Fig. 1, indicates that the fragmentation is done for coordinate α covering two adjacent subranges: [0,30] both [30,60], and v coordinate covering two adjacent subranges: [2.5,5.0] and [5.0,7.5]. The regrouping of data for the 4 selected fragments has allowed constructing Table 3.

The data for each fragment in Table 3 are processed by the CRA mathematical method, which receives polynomials of the second and third order. The approximation of the fragments with the polynomials of the second order leads to too high approximation error of the experimental points, respectively for the described fragments: 1–8%, 2–8.1%, 3–5.7%, 4–12.3%. The approximation of the same data polynomials of the third order provides approximately twice higher precision: 1–4.1%, 2–5.7%, 3–2.6%, 4–5.1%. Further increase in the accuracy applying the polynomial approximation is only possible by applying special methods, since the

Table 3 The fragmented dependency of the airship side shift force resulting from the flight parameters

Fragment 1				Fragment 2				Fragment 3				Fragment 4			
x_1	x_2	x_3	F_x	x_1	x_2	x_3	F_x	x_1	x_2	x_3	F_x	x_1	x_2	x_3	F_x
α	h	v	F_x	α	h	v	F_x	α	h	v	F_x	α	h	v	F_x
dgr	km	m/s	kN	dgr	km	m/s	kN	dgr	km	m/s	kN	dgr	km	m/s	kN
0	5	2.5	0.05	0	5	5	0.208	30	5	2.5	19.116	30	5	5	67.394
15	5	2.5	6.996	15	5	5	26.466	45	5	2.5	13.026	45	5	5	52.482
30	5	2.5	19.116	30	5	5	67.394	60	5	2.5	5.422	60	5	5	23.086
0	10	2.5	0.027	0	10	5	0.113	30	10	2.5	10.387	30	10	5	42.766
15	10	2.5	4.193	15	10	5	22.482	45	10	2.5	7.234	45	10	5	28.839
30	10	2.5	10.387	30	10	5	42.766	60	10	2.5	3.081	60	10	5	12.303
0	15	2.5	0.012	0	15	5	0.051	30	15	2.5	4.707	30	15	5	17.718
15	15	2.5	1.957	15	15	5	7.841	45	15	2.5	3.382	45	15	5	13.774
30	15	2.5	4.707	30	15	5	17.718	60	15	2.5	1.435	60	15	5	5.482
0	5	4	0.132	0	5	6	0.3	30	5	4	47.445	30	5	6	96.682
15	5	4	20.437	15	5	6	36.707	45	5	4	33.852	45	5	6	77.616
30	5	4	47.445	30	5	6	96.682	60	5	4	14.265	60	5	6	32.76
0	10	4	0.071	0	10	6	0.166	30	10	4	27.238	30	10	6	60.821
15	10	4	12.301	15	10	6	22.962	45	10	4	18.537	45	10	6	41.879
30	10	4	27.238	30	10	6	60.821	60	10	4	8.056	60	10	6	19.966
0	15	4	0.032	0	15	6	0.074	30	15	4	11.368	30	15	6	25.564
15	15	4	5.01	15	15	6	11.352	45	15	4	8.684	45	15	6	19.889
30	15	4	11.368	30	15	6	25.564	60	15	4	3.53	60	15	6	8.192
0	5	5	0.208	0	5	7.5	0.48	30	5	5	67.394	30	5	7.5	133.135
15	5	5	26.466	15	5	7.5	79.174	45	5	5	52.482	45	5	7.5	123.261
30	5	5	67.394	30	5	7.5	133.135	60	5	5	23.086	60	5	7.5	50.858

(continued)

Table 3 (continued)

Fragment 1				Fragment 2				Fragment 3				Fragment 4			
x_1	x_2	x_3	F_x	x_1	x_2	x_3	F_x	x_1	x_2	x_3	F_x	x_1	x_2	x_3	F_x
α	h	v	F_x	α	h	v	F_x	α	h	v	F_x	α	h	v	F_x
dgr	km	m/s	kN	dgr	km	m/s	kN	dgr	km	m/s	kN	dgr	km	m/s	kN
0	10	5	0.113	0	10	7.5	0.261	30	10	5	42.766	30	10	7.5	84.9
15	10	5	22.482	15	10	7.5	42.743	45	10	5	28.839	45	10	7.5	66.4
30	10	5	42.766	30	10	7.5	84.9	60	10	5	12.303	60	10	7.5	28.035
0	15	5	0.051	0	15	7.5	0.117	30	15	5	17.718	30	15	7.5	44.902
15	15	5	7.841	15	15	7.5	18.24	45	15	5	13.774	45	15	7.5	30.755
30	15	5	17.718	30	15	7.5	44.902	60	15	5	5.482	60	15	7.5	13.344

number of data for each fragment is equal to 27. The size of the full polynomial of the third order makes 20 members, and the size of the full polynomial of the fourth order makes 35 members. Therefore, further increase in accuracy of the approximation by increasing the polynomial order is impossible, and in this example, the order of the approximation is limited to the third order with the worst accuracy of 5.7%, as determined by the third fragment. Thus, FAF for all the fragments has an identical structure:

$$F_x^p(x) = \beta_0^p + \sum_{i=1}^{3} \beta_i^p \cdot x_i + \sum_{i=1,j=1}^{3} \beta_{ij}^p \cdot x_i \cdot x_j + \sum_{i=1,j=1,k=1}^{3} \beta_{ijk}^p \cdot x_i \cdot x_j \cdot x_k; k = \overline{1.4}. \tag{15}$$

The 3-dimensional 3-MVF is constructed, as shown above, on the base of 1-MCF with the intervals, which are predefined. According to the structure of n-IMF, and according to formula (7) all four 3-MCF for the isolated fragments are defined by the common expression, having the following form:

$$\lambda_{(i_1,i_2i_3)}\left(\vec{x}, \vec{x}_{(i_1-1,i_2-1,i_3-1)}, \vec{x}_{(i_1,i_2i_3)}, \varepsilon\right) = \prod_{p=1}^{3} \lambda_{p_i}\left(x_p, x_{p_{i-1}}, x_{p_i}, \varepsilon\right), \tag{16}$$

here $i_1 = \overline{1,2}; i_2 = 1; i_3 = \overline{1,2}; \vec{x} = (x_1, x_2, x_3)'; x_{1_{10}} = 0°; x_{1_{11}} = x_{1_{20}} = 30°; x_{1_{21}} = 60°;$ $x_{2_{10}} = 5.0\,\text{km}; x_{2_{11}} = 15.0\,\text{km}; x_{3_{10}} = 2.5\,\text{m/s}; x_{3_{11}} = x_{3_{20}} = 5.0\,\text{m/s}; x_{3_{21}} = \text{m/s}.$

The applied IIF of the fragments are defined according to Eq. (8), as follows:

$$f_{(1,1,1)}(\vec{x}) = \varphi_{(1,1,1)}(\vec{x}) \cdot \lambda_{(1,1,1)}\left(\vec{x}, \vec{x}_{(0,0,0)}, \vec{x}_{(1,1,1)}, \varepsilon\right), \tag{17.1}$$

$$f_{(1,1,2)}(\vec{x}) = \varphi_{(1,1,2)}(\vec{x}) \cdot \lambda_{(1,1,2)}\left(\vec{x}, \vec{x}_{(0,0,1)}, \vec{x}_{(1,1,2)}, \varepsilon\right), \tag{17.2}$$

$$f_{(2,1,1)}(\vec{x}) = \varphi_{(2,1,1)}(\vec{x}) \cdot \lambda_{(2,1,1)}\left(\vec{x}, \vec{x}_{(1,0,0)}, \vec{x}_{(2,1,1)}, \varepsilon\right), \tag{17.3}$$

$$f_{(2,1,2)}(\vec{x}) = \varphi_{(2,1,2)}(\vec{x}) \cdot \lambda_{(2,1,2)}\left(\vec{x}, \vec{x}_{(1,0,1)}, \vec{x}_{(2,1,2)}, \varepsilon\right), \tag{17.4}$$

where values of indices in the brackets are specifying the coordinate number of the fragment: the first and third index specify the numbers of α angle of heel fragments and v speeds, respectively, and the coordinate number for 'h' as the second index, which does not change, since the fragments belong to all the range of this variable.

The total EAF is formed according to Eq. (14), where the additive expression has the following form:

$$f(\vec{x}) = f_{(1,1,1)}(\vec{x}) + f_{(1,1,2)}(\vec{x}) + f_{(2,1,1)}(\vec{x}) + f_{(2,1,2)}(\vec{x}), \tag{18}$$

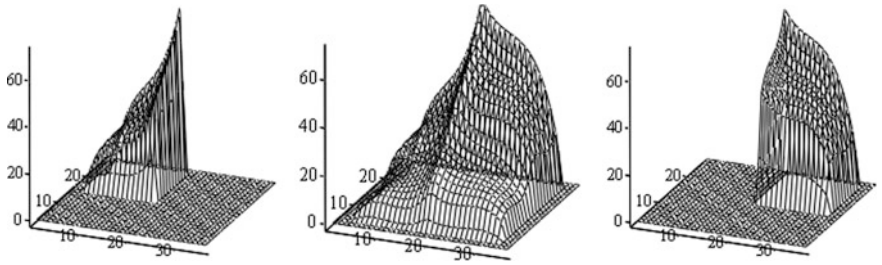

Fig. 4 The 2 of 4 IIF, and the total EAF (sections for h = x_2 = 10 km)

The analysis of EAF (17.1–17.4) has shown that the module of the greatest approximation error of this united function (5.64%) does not exceed the greatest fragments error (5.7%). The check is made for the wide range of values $\varepsilon \in [0.01–0.10]$. It confirms operability of the cut-glue approximation method for the 3-dimensional data.

In Fig. 4, the 3D-images illustrating the isolation stages of IIF from the corresponding FAF are shown. In addition the result of the association of the four IIF in EAF is shown too. Due to the impossibility of an evident illustration of the received 3-dimensional dependencies coming from 4-dimensional space, in Fig. 4, the projections of the constructed 4-dimensional figures are representing 3-dimensional subspace formed by independent variables $x_1 - \alpha$ and $x_3 - v$, and also the F_x output variable, called "sections".

10 Conclusion

1. The research on the mathematical models and algorithms defining the main stages of the cut-glue approximation method of the multidimensional experimental data has been shown, indicating the possible applications of this method, as the viable solution in approximating n-dimensional problems.
2. For the first time, this conclusion is illustrated, by showing the solution of a problem requiring the approximation of 3-dimensional dependences, based on the experimental data from the performed research in designing a real airship.
3. This research has accomplished all the stages of the cut-glue approximation method with the multidimensional experimental data, and showed high performance with the mixed computer and manual methods resources for the data processing, when approximating higher than 2-dimensions.
4. The final conclusion shows the urgent need to formalize the algorithms for all stages of the studied method, and their full automation, in order to ensure a broad and universal application of the CGA method for tackling the multidimensional approximation problems.

References

1. Loran P (1975) Approximation and optimization. Trans with English, World, Moscow, 496p
2. Insung I, Naylor B (1990) Piecewise linear approximations of digitized space curves with applications. Computer Science Technical Reports. Report Number: 90-1036. Paper 37. http://docs.lib.purdue.edu/cstech/37. Accessed 12 Jul 2016
3. António M, Pinheiro G, Ghanbari M (2010) Piecewise approximation of contours through scale-space selection of dominant points. IEEE Trans Image Process 19(6). doi:10.1109/TIP.2010.2043008
4. Ahlberg J, Nilson E, Walsh J (1967) The theory of splines and their applications. Academic Press, New York
5. De Boor C (1978) A practical guide to splines. Springer, New York
6. Micula G, Micula S (1999) Handbook of splines. Kluwer Academic Publishers, Dordrecht
7. Rawlings J, Pantula S, Dickey D (1998) Applied regression analysis: a research tool, 2nd edn. Springer, New York, 671p. ISBN 0-387-98454-2, SPIN 10660129
8. Bates D, Watts D (1988) Nonlinear regression analysis and its applications. Wiley, New York, p 365
9. Drapper N, Smith J (1981) Applied regression analysis, vol 1. Wiley, New York, p 366
10. Drapper N, Smith J (1981) Applied regression analysis, vol 2. Wiley, New York, p 351
11. Vilmos T (2005) Orthogonal polynomials. In: Surveys in approximation theory. pp. 70–125, vol 1, ISSN 1555-578X
12. Khrushchev S (2008) Orthogonal polynomials and continued fractions from Euler's point of view. Atilim University, Turkey: Cambridge University Press, www.cambridge.org/9780521854191. Accessed 12 Jul 2016
13. Powell M (1992) The theory of radial basis function approximation. In: Light W (ed) Advanced numerical analysis, vol II. OUP, Oxford University Press, Oxford, pp 105–210
14. Sarra S, Kansa E (2009) Multiquadric radial basis function approximation methods for the numerical solution of partial differential equations. Marshall University and University of California, Davis, June 30, 220p. www.ScottSarra.org/math/math.html. Accessed 13 Jul 2016
15. Buhmann M (2003) Radial basis functions: theory and implementations. Cambridge University Press, Cambridge. http://www.math.ucdavis.edu/~saito/data/jim/buhmann-actanumerica.pdf. Accessed 13 Jul 2016
16. Neydorf R (2014) Approximating creation of mathematical models on dot experimental data by cut-glue method. DSTU Bull 14(75)45–58
17. Neydorf R (2014) "Cut-Glue" approximation in problems on static and dynamic mathematical model development. Proc ASME Intl Mechan Eng Congr Expos (IMECE), 1. doi:10.1115/IMECE2014-37236
18. Neydorf R (2015) Bivariate "Cut-Glue" approximation of strongly nonlinear mathematical models based on experimental data. SAE Int J Aerosp 8(1):2015. doi:10.4271/2015-01-2394. http://papers.sae.org/2015-01-2394. Accessed 13 Jul 2016
19. Neydorf R, Sigida Y (2014) Identification of traction and power characteristics of air-screw propulsors in mathematical description of airship. SAE Technical Paper 2014-01-2134. doi:10.4271/2014-01-2134
20. Neydorf R, Sigida Y, Voloshin V, Chen Y (2013) Stability analysis of the MAAT feeder airship during ascent and descent with wind disturbances. SAE Technical Paper 2013-01-2111, 2013. doi:10.4271/2013-01-2111
21. Neydorf R, Neydorf A (2016) Technology of cut-glue approximation method for modeling strongly nonlinear multivariable objects. Theoretical Bases and Prospects of Practical Application, SAE Technical Paper 2016-01-2035, 2016. doi:10.4271/2016-01-2035
22. Pshikhopov V, Medvedev M, Gaiduk A, Neydorf R et al (2013) Mathematical model of robot on base of airship. In: 52nd conference on decision and control, Florence, Italy, 10–13 Dec 2013. Proceedings of the IEEE conference on decision and control, p 959

23. Pshikhopov V, Medvedev M, Neydorf R, Krukhmalev V, Kostjukov V, Gaiduk A, Voloshin V (2012) Impact of the feeder aerodynamics characteristics on the power of control actions in steady and transient regimes. SAE Technical Paper 2012-01-2112. doi:10.4271/2012-01-2112
24. Voloshin V, Yong Ch, Neydorf R, Boldyreva A (2013) Aerodynamic characteristics study and possible improvements of MAAT feeder airships. SAE Technical Paper 2013-01-2112. doi:10.4271/2013-01-2112
25. Osiaev OG (2010) Resource-saving forecasting method of long durability of polymeric materials in case of multiple-factor loading. In: Osiaev OG, Neydorf RA (eds) Reviews of SFU. Technical science. Thematic release "Methods and means of adaptive management in power". TTI SFU Publishing House, Taganrog, vol 1, no 102. http://izv-tn.tti.sfedu.ru/wp-content/uploads/PDF/2010_1(102).pdf. Accessed 14 July 2016
26. Osiaev OG (2010) The formalized analysis of settlement cases of loading and resource of operation of aircraft. In: Osiaev OG, Neydorf RA (eds) Control systems and information technologies, vol 2, no 40. Scientific Book Publishing House, Moscow, Voronezh. http://www.sbook.ru/suit/contents/100200.pdf. Accessed 14 Jul 2016
27. Osiaev OG (2010) Numerical forecasting method of the difficult stress-strain state of designs of flight vehicles. Reviews of SFU. Technical science. Thematic release: "Perspective systems and tasks of control". TTI SFU Publishing House, Taganrog, vol 3, no 104. http://izv-tn.tti.sfedu.ru/wp-content/uploads/2010/3/35.pdf. Accessed 15 Jul 2016
28. Pshikhopov V, Medvedev M, Gaiduk A, Neydorf R et al (2013) System of position and trajectory management of a robotic aeronautic platform: mathematical model. Mechatron Autom Control 6:14–21. http://novtex.ru/mech/mech2013/Mh613_web.pdf. Accessed 15 July 2016
29. Pshikhopov V, Medvedev M, Gaiduk A, Neydorf R et al. (2013) System of position and trajectory management of a robotic aeronautic platform: control algorithms. Mechatron Autom Control 7:13–20. http://novtex.ru/mech/mech2013/Mh713.pdf
30. Neydorf R, Novikov S, Fedorenko R (2013) Continuous-positional automatic ballonet control system for airship. 2013 SAE Intl J Aerosp 6(2). ISSN: 1946-3855
31. Neydorf R, Novikov S, Kudinov N (2014) Airship positioning fuzzy multi-ballonet control study. SAE Technical Paper 2014-01-2146, 2014. doi:10.4271/2014-01-2146